Supporting information for the manuscript

Does Tyrosine Protect *S. coelicolor* Laccase from Oxidative Degradation or Act as an Extended Catalytic Site?

Patrycja J. Kielb[1]*†, Christian Teutloff[2], Robert Bittl[2], Harry B. Gray[1]*, Jay R. Winkler[1]*

[1]Beckman Institute, California Institute of Technology, Pasadena CA 91125, United States
[2]Department of Physics, Freie Universität Berlin, 14195 Berlin, Germany

Content

1. Materials and methods

Protein expression and purification:

The lyophilized plasmid containig the tSLAC gene (residues 45-343) was resuspended in EB buffer and diluted to a final concentration of 10 ng/μL. The diluted pET28b(+) strain was transformed into competent NovaBlue cells, which were subsequently grown overnight at 37°C. The next day, single colonies were chosen for inoculation (12-16 h at 37°C, shaking at 250 RPM) in 5 mL of LB media supplemented with kanamycin antibiotic at a concentration of 50 μg/mL. After cells were grown, the DNA was extracted and purified using a MiniPrep kit from Millipore. After DNA verification, the plasmid solutions were used for transformation into BL21 (DE3) cells. Cells were distributed into a Petri dish containing LB medium supplemented with kanamycin antibiotic and were incubated overnight (12-16h) at 37 °C, shaking at 250 RPM. The next day, single colonies were chosen for inoculation (*ca.* 6 h at 37 °C, shaking at 250 RPM) in 5 mL of TB medium supplemented with kanamycin antibiotic. After that time, grown cells were transferred into 6-L Erlenmeyer flasks and further grown in 2L of autoclaved TB medium with kanamycin. The cells were grown at 30 °C, shaking at 190 RPM until an optical density at 600 nm (OD_{600nm}) reached a value of 0.6-1.0.

Protein expression was induced by adding 0.4 mM of Isopropyl-β-D-1-thiogalactopyranoside (IPTG) to the cell media. At the same time, 0.6 mM of $CuSO_4$ was added to cell culture to induce SLAC metalation during folding, as shown in a similar protocol for of expression and metalation of CotA laccase by Durao et al.[1] After 4 h of shaking at 170 RPM (25 °C), the cell culture was incubated at RT for another 20 h without shaking. Metal content analysis of purified expressed protein exhibited higher copper content (~3.9 Cu/monomer) than that of protein in which Cu was incorporated via dialysis against copper salts after protein purification.

Cells were harvested by centrifugation. Pellets were resuspended in 10 mM sodium phosphate buffer pH 7.5 with 250 mM NaCl and 10 mM imidazole. Cell contents were released using sonication by applying six cycles of 5 min of repeated 1-s sonication and 1-s waiting time steps. During sonication, the protein solution was stored in an ice bath. The obtained lysate was centrifuged for 45 min at 12000 RPM to separate protein extracts from residual of the cell media. The supernatant was filtered through 0.22 mm filters.

The filtrate was used as starting material in the three-step SLAC purification procedure. First, affinity chromatography with Ni-NTA beads was used to separate HisTag-SLAC from other proteins. The solution was loaded onto a washed and pre-equilibrated column with 10 mM phosphate pH 7.5 buffer containing 300 mM NaCl and 10 mM imidazole. The bound protein was washed with equilibration buffer and then

with a washing buffer containing 30 mM of imidazole. The protein was eluted from the column using 10 mM phosphate pH 7.5 buffer containing 300 mM NaCl and 300 mM imidazole. Eluted fractions with blue color, indicative of Cu_{T1}^{2+} of laccase, were collected and loaded onto 10 kDa or 30 kDa spin-filters, washed and centrifuged for multiple cycles until the concentration of imidazole decreased to *ca.* 30 mM. The concentrated protein solution was diluted with equilibration buffer and loaded onto a Ni-NTA column for the second time. The purification protocol, as described above, was repeated with the difference of washing buffer used, which contained 50 mM imidazole in the second run. After elution, NaCl and imidazole were removed from the solution using spin-filters. The next step of purification employed FPLC anion exchange chromatography.[2] The protein solution (10 mM phosphate pH 7.5) was loaded onto the pre-equilibrated (10 mM phosphate pH 7.5) diethylaminoethyl–Sepharose (HiTrap DEAE Sepharose FF 3×5 mL column, GE HealthCare) column. The loaded protein was washed with the same buffer and eluted with a gradient of 0-500 mM NaCl. The protein began to elute at ca. 100-200 mM NaCl and blue fractions were pooled. The protein concentration was assessed by UV-Vis spectroscopy determining the absorbance at 280 nm (Gill-Hippel assay).[3] The protein solution was stored at - 80°C in the presence of 20-30% of glycerol. Mass spectrometry indicated a mass of 32256 Da (WT), which corresponds to His-TagSLAC protein without the last three residues (EPH). All other SLAC variants (W284F, W132F, and Y108F) were prepared in the same way.

Metal content analysis:

A modified BCA (bicinchoninic acid) assay was used to analyze copper content in purified samples.[4,5] In the first step, the protein was denatured by mixing 30 μL of 100 μM of protein solution with 45 μL of 10 M urea. The pH was adjusted to 3.5 with trichloroacetic acid to prevent the Biuret reaction. The solution was left overnight at RT. Subsequently, released copper ions from the protein were reduced by the addition of L-ascorbic acid. The BCA reagent (ThermoScientitc ™ Pierce™)[6] was then added to the protein solution to chelate Cu^{1+} ions. The copper concentration was assessed by the absorbance of Cu-BCA molecules at 568 nm in comparison to a previously prepared calibration curve. SLAC samples were found to house around 3.9 copper atoms per monomer.

Site-directed mutagenesis:

Primers for Y108F mutation:

Y108F-F 5'-CAC GGC CTG GAC TAC GAG ATC TCC AGC-3'

Y108F-R 5'-GCT GGA GAT CTC GAA GTC CAG GCC GTG-3'

Primers for W132F mutation:

W132F-F 5'-CGC ACC TAC ACC TTC CGC ACC CAC AAA C-3'

W132F-R 5’-G TTT GTG GGT GCG GAA GGT GTA GGT GCG-3’

Primers for W284F mutation:

W284F-F 5'-GGC GCC GGG GCG TTC ATG TAC CAC TGC-3'

W284F-R 5'-GCA GTG GTA CAT GAA CGC CCC GGC GCC-3'

Primers for C288S (T1D) mutation:

C288S-F 5' (TGG ATG TAC CAC AGC CAC GTC CAG AGC CAC)

C288S-R 5' (GTG GCT CTG GAC GTG GCT GTG GTA CAT CCA)

The last primers (C288S) were used to create a double mutant with C288S and W132F mutations.

DNA sequencing and mass spectroscopy confirmed successful site-directed mutagenesis of all SLAC variants.

2. Electron transfer map using https://emap.bu.edu

We have used software (www.emap.bu.edu)[7] developed by the Bravaya group to identify possible ET pathways in SLAC. The computations based on the semiclassical electron-transfer theory[8] and implemented with a *Pathways* model developed by D. Beratan and coworkers.[9,10] The software generated an ET map employing all possible aromatic residues meeting a 'pairwise distance' criteria, based on the available crystal structure (pdb id: 3CG8). We focused on identifying possible pathways originating from the Y108 residue and obtained three possibilities shown below (Figures S1- S3).

The representation of the first pathway Y108-W132-...-Y54 ending with surface-exposed Y54 residue is presented on Figure S1. The shortest pathway includes residues Y108, W132, Y130, and Y54. Other possible ET routes include Y155, Y65, and Y174.

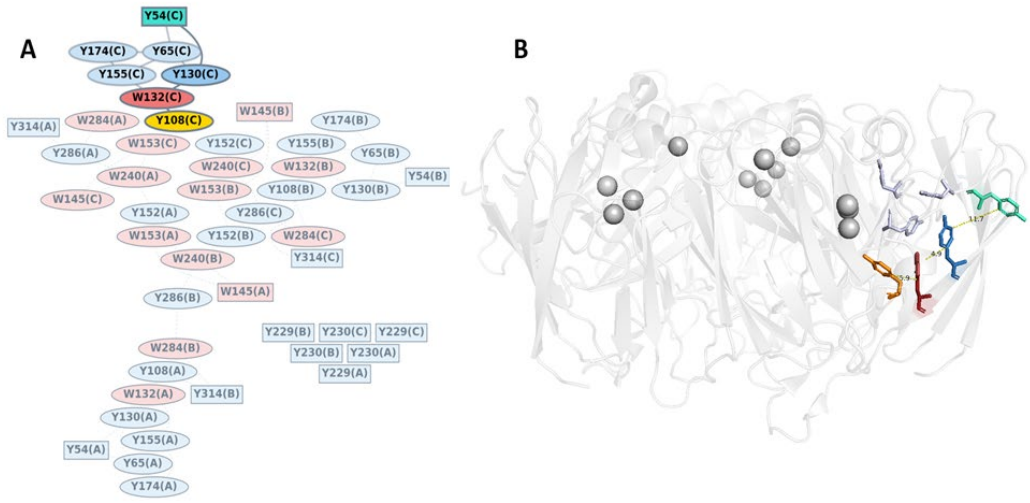

Figure S1. ET map analysis generated by eMap software on SLAC structure (pdb id: 3cg8). (A) The ET map representing all possible aromatic residues with the indicated shortest path from Y108 (chain C) to Y54 (chain C), marked in yellow and green, respectively. (B) The 3D structure of the analyzed ET pathway.

The representation of the second pathway Y108-W284-…-Y314 ending with surface-exposed Y314 residue is presented on Figure S2. The shortest pathway includes residues Y108, W284, (Y286), and Y314.

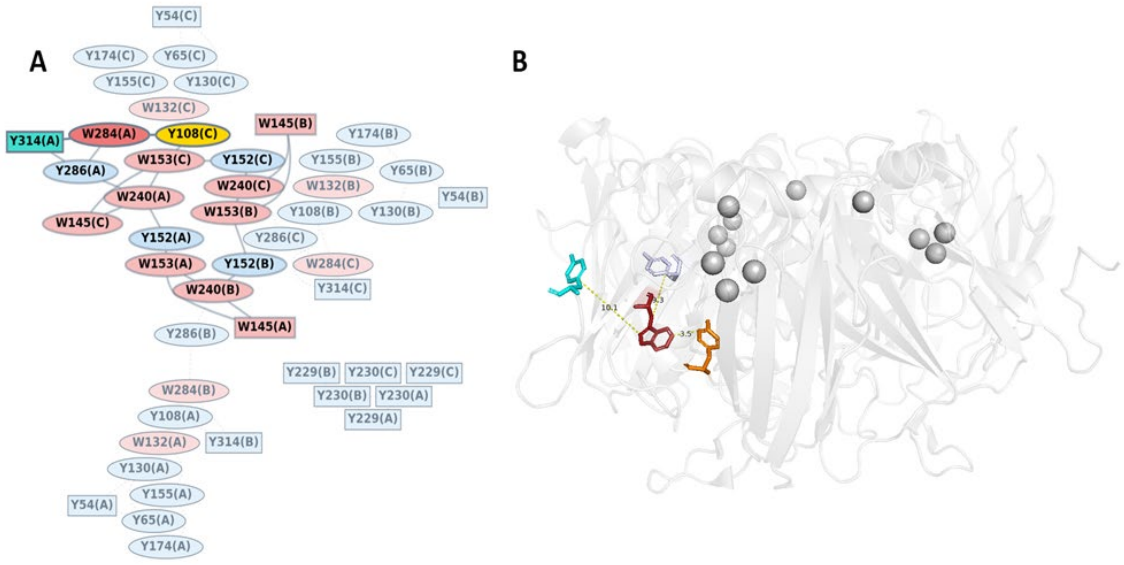

Figure S2. ET map analysis generated by eMap software on SLAC structure (pdb id: 3cg8). (A) The ET map representing all possible aromatic residues with the indicated shortest path from Y108 (chain C) to Y314 (chain A), marked in yellow and green, respectively. (B) The 3D structure of the analyzed ET pathway.

The representation of the third pathway Y108-W153-...-W145 ending with surface-exposed W145 residue is presented on Figure S3. The distance between Y108 and the second residue in the path (W153) is longer than 9 Å, which makes it less likely for the electron to be transferred from one to another via hole hopping mechanism. Moreover, the path involves many more residues than previous ones, resulting in a relatively long path (37 Å). On the basis on these consideratons, we excluded this pathway as a potential radical transfer route from Y108 to the protein surface.

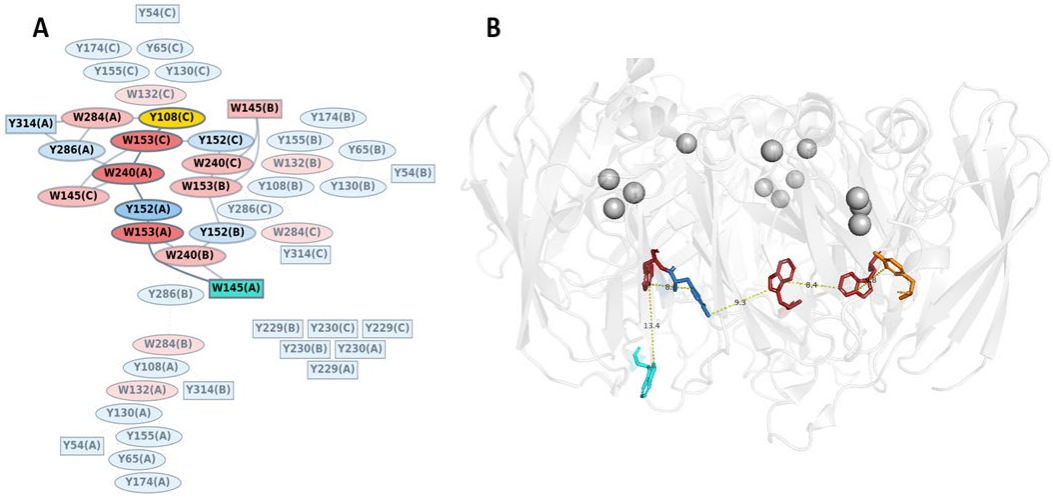

Figure S3. ET map analysis generated by eMap software on SLAC structure (pdb id: 3cg8). (A) The ET map representing all possible aromatic residues with the indicated shortest path from Y108 (chain C) to Y145 (chain A), marked in yellow and green, respectively. (B) The 3D structure of the analyzed ET pathway.

3. Steady-state Michaelis-Menten kinetics

One-electron oxidation of $ABTS^{2-}$ forms a radical $ABTS^{\bullet-}$ with distinct absorbance features at 420 nm and broad band at 600-800 nm (Figure S4). We have monitored a change in absorbance of $ABTS^{\bullet-}$ at 420 nm, (ε_{420}=36000 $M^{-1}cm^{-1}$) in 100 μM-10mM $ABTS^{2-}$ solutions heated to 60 °C at pH 4.5 with O_2 concentration of ca. 270 μM, as a function of time after the addition of 25 nM of SLAC variants. The observed time traces were corrected for uncatalyzed $ABTS^{2-}$ oxidation by subtraction of a trace obtained in the absence of enzyme.

Initial enzymatic kinetic rates were calculated from obtained data and plotted against $ABTS^{2-}$ concentration (Figure S5). Data were fit to the Michaelis-Menten (MM) equation from which Michaelis-Menten constants (K_m) and catalytic rate constants (k_{CAT}) were calculated (Table S1). A minimal representation of the Michaelis-Menten model describing SLAC kinetics is depicted on the Figure S6. It is interesting to note that k_{CAT} values are similar in all SLAC variants, but K_M values differ. While W132F gives the highest K_M value, W284F gives the lowest K_M value and the best catalytic performance as its catalytic efficiency (k_{CAT}/K_M) is 1.5 times higher than for the WT (Figure S5 and Table S1). Based on the MM model, it is reasonable to consider these changes as a result of either different kinetic rates of substrate binding (k_1) or different rates of oxygen reduction kinetics (Figure S6). It is unlikely that the former contributes to these differences as mutations are not nearly close to the substrate-binding pocket. As for the latter, oxygen reduction kinetics are greatly oversimplified in the MM model, making it very difficult to receive any reliable information about this process, that could be drawn from a comparison among samples. However, all SLAC variants remain catalytically active upon single mutations, as evident by their higher catalytic rates than in studies published by Sherif et al. in which $ABTS^{2-}$ has been used as a substrate in similar conditions.[11]

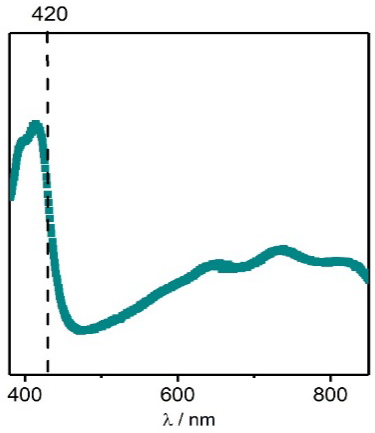

Figure S4. The UV-Vis spectrum of $ABTS^{\bullet-}$ radical in 100 mM acetate buffer pH 4.5 obtained by one-electron oxidation of $ABTS^{2-}$ by SLAC in the presence of oxygen. Changes in absorbance at 420 nm were monitored as a measure of $ABTS^{2-}$ oxidation.

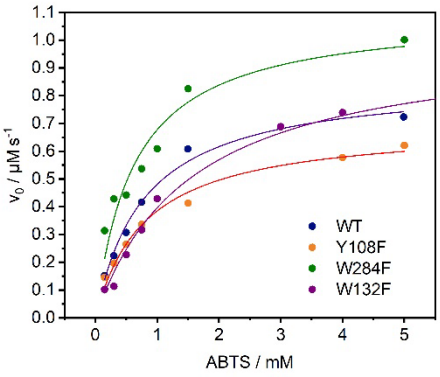

Figure S5. Rate of $ABTS^{2-}$ oxidation by SLAC variants (WT – navy blue, Y108F – orange, W284F – green, W132F – purple) plotted against $ABTS^{2-}$ concentration (0.1 – 5 mM) measured in acetate buffer pH 4.5 at 60 °C and 270 µM of O_2. Dotted lines represent data, and solid lines represent the fitted Michaelis-Menten model from which further parameters were derived.

Figure S6. The simplistic representation of the Michaelis-Menten model used for analyzing SLAC's enzymatic kinetics. E_{OX} stands for an oxidized enzyme, E_{OX}-ABTS represents Enzyme-Substrate (ES) complex, and E_{RED} is a reduced enzyme.

Table S1. Michaelis- Menten constant (K_M), rates of catalytic turnover (k_{CAT}), and second-order rate constants (k_{CAT}/K_M) of WT, Y108F, W132F, and W284F SLAC variants, derived from Michaelis-Menten experiments and analysis according to $K_M = \frac{k_{-1}+k_2}{k_1}$, $k_{CAT} = k_2$. *Data refer to published results by Sherif at al.[11], who evaluated catalytic parameters of WT using ABTS as a subtrate at pH 4.0 and at 60 °C.

	K_M / mM	k_{CAT} /s^{-1}	k_{CAT}/K_M / $M^{-1}s^{-1}$
WT	0.98 ± 0.3	36 ± 7	(3.7±0.6) × 10^4
Y108F	1.07 ± 0.3	32 ± 5	(3.0±0.4) × 10^4
W132F	1.33 ± 0.3	38 ± 4	(2.9±0.2) × 10^4
W284F	0.6 ± 0.02	35 ±3	(5.8±0.3) × 10^4
***WT (Sherif et al.)**	0.8	7.7	1 × 10^4

4. Single oxygen turnover by SLAC variants experiments.

Table S2. The initial concentrations of reagents used in single-oxygen turnover experiments.

	[Protein] / μM	[O_2] / μM	[Asc] / μM
WT	145	40	1153
W284F	76.5	31	680
W132F	190	70	710
Y108F	57	52	900

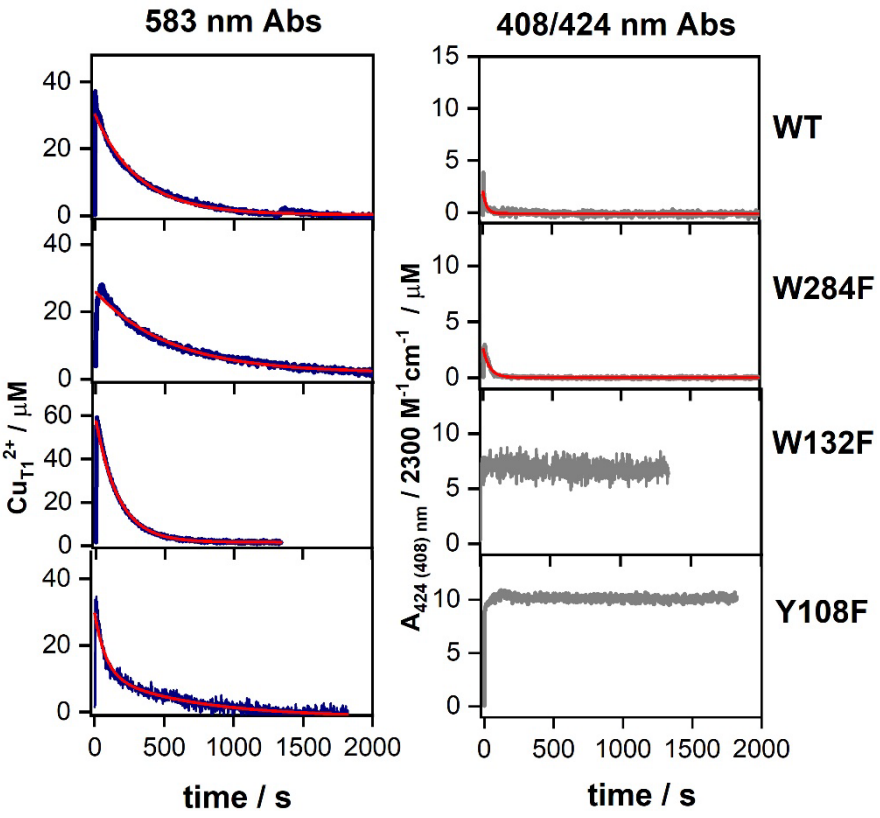

Figure S7. Time traces of concentration of Cu_{T1}^{2+} (left) and $Tyr_{108}^{\bullet}$ and 408 nm absorbance (right) in SLAC variants, calculated from spectral intensities of 583 nm and either 408 nm or 424 nm peaks, are shown as blue and grey lines, respectively fitted to mono or bi-exponential decay functions (red lines).

Table S3. Time constants and amplitudes obtained from exponential fits in Figure S7.

	Decay of 583 nm absorbance	Decay of 424 nm absorbance
WT	t = 317 s A = 31	t = 9 A = 4.2
W284F	t = 538 s A = 24	t = 43 s A = 3
W132F	t = 153 s A = 59	-
Y108F	t_1 = 671 s A_1 = 13 t_2 = 80 s A_2 = 18	-

5. EPR measurements.

A Cu_{T1}-depleted (T1D) W132F SLAC sample for the EPR measurements was prepared in the same way as samples for the single-oxygen turnover kinetic experiments described above. The deoxygenated protein solution (180 μM) was mixed with the deoxygenated ascorbic acid solution until SLAC was completely reduced. Subsequently, the SLAC-ascorbic acid solution was mixed with oxygenated 10 mM phosphate pH 7.5 buffer containing glycerol, transferred to an EPR tube, and rapidly frozen in liquid nitrogen. The time between the addition of oxygenated solution to fully frozen sample was approximately 2 mins.

X-band CW EPR spectra of the T1D W132F sample were acquired at Caltech on a Bruker (Billerica, MA) EMX spectrometer using Bruker Win-EPR software (ver. 3.0). Temperature control was achieved using liquid helium and an Oxford Instruments (Oxford, UK) ESR-900 cryogen flow cryostat and an ITC-503 temperature controller. The EPR spectrum was recorded at 40 K, at 9.64 GHz microwave frequency with 2.036 mW microwave power and 8 G modulation amplitude and 20.48 ms of conversion time. 40 scans were recorded and averaged (Figure S8).

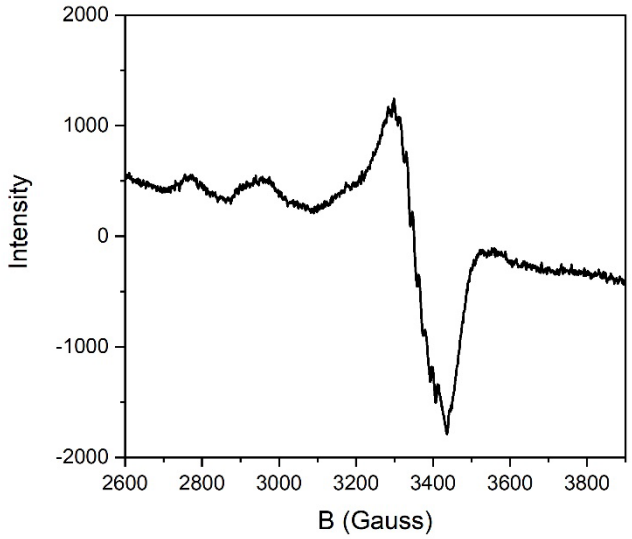

Figure S8. The X-band EPR spectrum of T1D W132F SLAC variant, recorded at 40K, at 9.64 GHz microwave frequency with 2.036 mW microwave power and 8 G modulation amplitude.

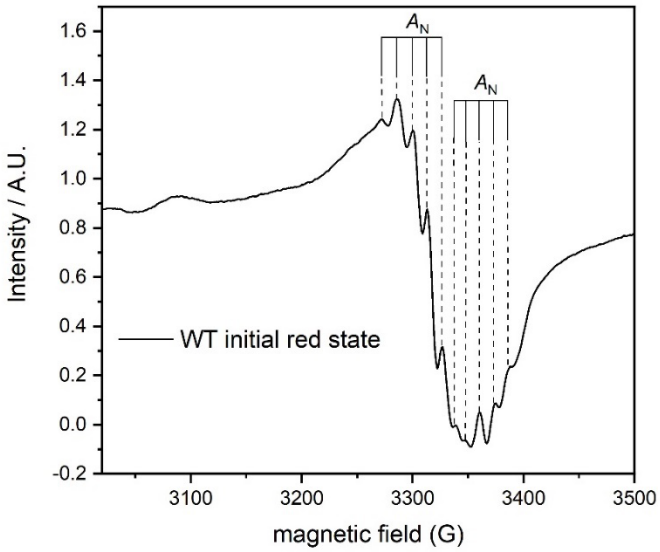

Figure S9. The X-band EPR spectrum of WT SLAC in the initial ascorbate-reduced state, recorded at 40K, at 9.39 GHz microwave frequency with 4.0 mW microwave power and 4 G modulation amplitude.

6. References

(1) Durão, P.; Chen, Z.; Fernandes, A. T.; Hildebrandt, P.; Murgida, D. H.; Todorovic, S.; Pereira, M. M.; Melo, E. P.; Martins, L. O. Copper Incorporation into Recombinant CotA Laccase from Bacillus Subtilis: Characterization of Fully Copper Loaded Enzymes. *J. Biol. Inorg. Chem.* **2008**, *13* (2), 183–193. https://doi.org/10.1007/s00775-007-0312-0.

(2) Gallaway, J.; Wheeldon, I.; Rincon, R.; Atanassov, P.; Banta, S.; Barton, S. C. Oxygen-Reducing Enzyme Cathodes Produced from SLAC, a Small Laccase from Streptomyces Coelicolor. *Biosens. Bioelectron.* **2008**, *23* (8), 1229–1235. https://doi.org/10.1016/j.bios.2007.11.004.

(3) Gill, S. C.; von Hippel, P. H. Calculation of Protein Extinction Coefficients from Amino Acid Sequence Data. *Anal. Biochem.* **1989**, *182* (2), 319–326. https://doi.org/10.1016/0003-2697(89)90602-7.

(4) Brenner, A. J.; Harris, E. D. A Quantitative Test for Copper Using Bicinchoninic Acid. *Analytical Biochemistry*. 1995, pp 80–84. https://doi.org/10.1006/abio.1995.1194.

(5) Huang, T.; Long, M.; Huo, B. Competitive Binding to Cuprous Ions of Protein and BCA in the Bicinchoninic Acid Protein Assay. *Open Biomed. Eng. J.* **2010**, *4*, 271–278. https://doi.org/10.2174/1874120701004010271.

(6) Thermo Scientific. User Guide: Pierce BCA Protein Assay Kit. *Pierce Biotechnol.* **2011**, *0747* (23225), 1–7. https://doi.org/10.1016/j.ijproman.2010.02.012.

(7) Tazhigulov, R. N.; Gayvert, J. R.; Wei, M.; Bravaya, K. B. EMap: A Web Application for Identifying and Visualizing Electron or Hole Hopping Pathways in Proteins. *J. Phys. Chem. B* **2019**, *123* (32), 6946–6951. https://doi.org/10.1021/acs.jpcb.9b04816.

(8) Marcus, R. A.; Sutin, N. Electron Transfers in Chemistry and Biology. *Biochim. Biophys. Acta - Rev. Bioenerg.* **1985**, *811* (3), 265–322. https://doi.org/10.1016/0304-4173(85)90014-X.

(9) Beratan, D. N.; Onuchic, J. N.; Winkler, J. R.; Gray, H. B. Electron-Tunneling Pathways in Proteins. *Science (80-.).* **1992**, *258* (5089).

(10) Onuchic, J. N.; Beratan, D. N.; Winkler, J. R.; Gray, H. B. Pathway Analysis of Protein Electron-Transfer Reactions. *Annu. Rev. Biophys. Biomol. Struct.* **1992**, *21*.

(11) Sherif, M.; Waung, D.; Korbeci, B.; Mavisakalyan, V.; Flick, R.; Brown, G.; Abou-Zaid, M.; Yakunin, A. F.; Master, E. R. Biochemical Studies of the Multicopper Oxidase (Small Laccase) from Streptomyces Coelicolor Using Bioactive Phytochemicals and Site-Directed Mutagenesis. *Microb. Biotechnol.* **2013**, *6* (5), 588–597. https://doi.org/10.1111/1751-7915.12068.